nature medicine

LETTERS

A live-attenuated Zika virus vaccine candidate induces sterilizing immunity in mouse models

Chao Shan[1], Antonio E Muruato[2,3], Bruno T D Nunes[1,4], Huanle Luo[5], Xuping Xie[1], Daniele B A Medeiros[1,4], Maki Wakamiya[1], Robert B Tesh[2,6], Alan D Barrett[2,6,7], Tian Wang[5,6,7], Scott C Weaver[2,3,5,7,8], Pedro F C Vasconcelos[4,9], Shannan L Rossi[2,6] & Pei-Yong Shi[1,7,8,10]

Zika virus (ZIKV) infection of pregnant women can cause a wide range of congenital abnormalities, including microcephaly, in the infant, a condition now collectively known as congenital ZIKV syndrome[1]. A vaccine to prevent or significantly attenuate viremia in pregnant women who are residents of or travelers to epidemic or endemic regions is needed to avert congenital ZIKV syndrome, and might also help to suppress epidemic transmission. Here we report on a live-attenuated vaccine candidate that contains a 10-nucleotide deletion in the 3′ untranslated region of the ZIKV genome (10-del ZIKV). The 10-del ZIKV is highly attenuated, immunogenic, and protective in type 1 interferon receptor–deficient A129 mice. Crucially, a single dose of 10-del ZIKV induced sterilizing immunity with a saturated neutralizing antibody titer, which no longer increased after challenge with an epidemic ZIKV, and completely prevented viremia. The immunized mice also developed a robust T cell response. Intracranial inoculation of 1-d-old immunocompetent CD-1 mice with 1×10^4 infectious focus units (IFU) of 10-del ZIKV caused no mortality, whereas infections with 10 IFU of wild-type ZIKV were lethal. Mechanistically, the attenuated virulence of 10-del ZIKV may be due to decreased viral RNA synthesis and increased sensitivity to type-1-interferon inhibition. The attenuated 10-del ZIKV was incapable of infecting mosquitoes after oral feeding of spiked-blood meals, representing an additional safety feature. Collectively, the safety and efficacy results suggest that further development of this promising, live-attenuated ZIKV vaccine candidate is warranted.

The mosquito-borne ZIKV has recently been recognized as a global public-health threat. Prevention of congenital ZIKV syndrome is the most pressing task to reduce the burden of Zika epidemics on families and society[2]. An effective vaccine is urgently needed for women of child-bearing age and travelers to endemic countries to prevent illness and suppress transmission. Both inactivated and live-attenuated vaccines have been developed for flaviviruses, including yellow fever (YFV), Japanese encephalitis (JEV), tick-borne encephalitis (TBEV), and dengue (DENV) viruses[3]. Rapid and promising progress has been made toward a ZIKV vaccine[4,5]. Inactivated ZIKV and subunit vaccines (expressing viral prM/E proteins) have shown efficacy in mice and nonhuman primates[6–10], but so far, there have been no reports of live-attenuated vaccine candidates. We chose to pursue a live-attenuated vaccine to capitalize on its advantages of single-dose immunization, rapid and robust immune response, and potentially long-lived protection. We attenuated wild-type (WT) ZIKV through deletion of the 3′ untranslated region (3′UTR) of the viral genome. A similar approach has been used successfully to develop a DENV vaccine, which is currently in a phase 3 clinical trial[11].

We used an infectious complementary DNA (cDNA) clone of the ZIKV Cambodian strain FSS13025 (ref. 12)—a nonepidemic strain that is phylogenetically closely related to those now circulating in the Americas—to prepare a panel of viruses containing distinct 3′UTR deletions (**Fig. 1a**). Mutant viruses 10-del, 20-del, 30-del-a, and 30-del-b contained overlapping 10-to-30-nucleotide deletions, which were expected to change the local RNA structure of the viral 3′UTR[13,14] (**Supplementary Fig. 1**). Upon transfection of these genomic RNAs into Vero cells, all mutated RNAs generated viral-E-protein-expressing cells (**Supplementary Fig. 2**) and infectious viruses (defined as P0 viruses). When compared to the WT virus, all mutated strains exhibited smaller infectious foci (**Fig. 1b**), slower replication kinetics, and lower peak titers (**Fig. 1c**). Next, we engineered the deletions into a luciferase ZIKV replicon to examine their roles in viral translation and RNA synthesis[15,16]. The replicon results showed that the 3′UTR deletions did not affect viral RNA translation, as indicated by the luciferase signals at 2–6 h post-transfection, but that there was modestly decreased RNA synthesis, as suggested by the luciferase

[1]Department of Biochemistry & Molecular Biology, University of Texas Medical Branch, Galveston, Texas, USA. [2]Institute for Human Infections & Immunity, University of Texas Medical Branch, Galveston, Texas, USA. [3]Institute for Translational Sciences, University of Texas Medical Branch, Galveston, Texas, USA. [4]Department of Arbovirology and Hemorrhagic Fevers, Evandro Chagas Institute, Ministry of Health, Ananindeua, Pará State, Brazil. [5]Department of Microbiology & Immunology, University of Texas Medical Branch, Galveston, Texas, USA. [6]Department of Pathology and Center for Biodefense & Emerging Infectious Diseases, University of Texas Medical Branch, Galveston, Texas, USA. [7]Sealy Center for Vaccine Development, University of Texas Medical Branch, Galveston, Texas, USA. [8]Sealy Center for Structural Biology & Molecular Biophysics, University of Texas Medical Branch, Galveston, Texas, USA. [9]Department of Pathology, Pará State University, Belém, Brazil. [10]Department of Phamarcology & Toxicology, University of Texas Medical Branch, Galveston, Texas, USA. Correspondence should be addressed to P.-Y.S. (peshi@utmb.edu) or S.L.R. (slrossi@utmb.edu).

Received 6 December 2016; accepted 9 March 2017; published online 10 April 2017; doi:10.1038/nm.4322

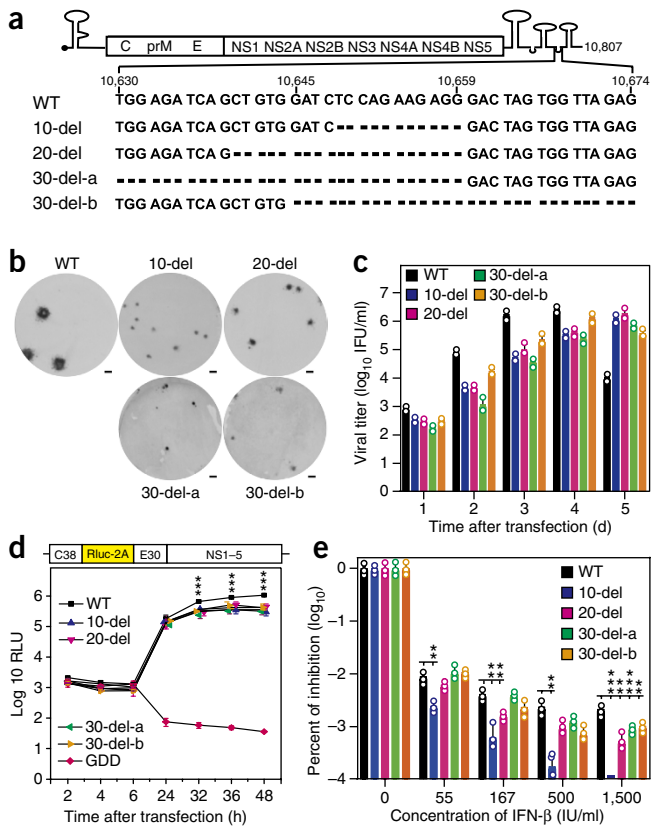

Figure 1 Characterization of the 3′UTR-deletion mutant viruses in cell culture. (**a**) Sequences of the ZIKV 3′UTR deletions. Deleted nucleotides are indicated by dashed lines. (**b**) Immunostaining focus assay of mutant viruses. Equal amounts of RNAs (10 μg) transcribed from their corresponding infectious cDNA clones were electroporated into Vero cells. On days 4 or 5 post-transfection, culture fluids from the transfected cells were harvested and quantified for infectious viruses (defined as P0 virus) by using an immunostaining focus assay on Vero cells. Scale bar, 1 mm. (**c**) Replication kinetics of WT and mutant viruses. Vero cells in 24-well plates (2×10^5 cells per well) were infected with WT and mutant viruses at a multiplicity of infection (MOI) of 0.01. Culture fluids were quantified for infectious viruses on days 1–5 using the immunostaining focus assay. (**d**) Replicon analysis of the 3′UTR deletions. A *Renilla* luciferase reporter replicon of ZIKV (top) was engineered with various 3′UTR deletions. Equal amounts of WT and mutant replicon RNAs (10 μg) were electroporated into Vero cells. Luciferase signals were measured at the indicated time points (bottom). A nonreplicative replicon containing an NS5 polymerase-inactive GDD-to-AAA mutation was included as a negative control. The averages of three replicates are presented. Error bars represent s.d. RLU, relative light units. (**e**) IFN-β inhibition of WT and mutant ZIKVs. Vero cells were seeded in a 96-well plate (1.5×10^4 cells per well) 1 d before interferon treatment and viral infection. The cells were infected at an MOI of 0.05 in the presence of indicated concentrations of IFN-β. Viral infection and interferon treatment were initiated at the same time. At 48 h after infection and IFN-β treatment, viral titers were quantified using the immunostaining focus assay on Vero cells. Percentages of viral titer inhibition are presented in $\log_{10}$ scale. Viral titers without IFN-β treatment are set as 100%. Average results of three independent experiments are shown. Error bars represent s.d. $^{**}P < 0.01$ and $^{***}P < 0.001$.

activity at 32–48 h post-transfection (**Fig. 1d**). Given that the 3′UTR of flaviviruses may also modulate the host innate immune response[17,18], we compared the susceptibility of the WT and mutated viruses to interferon treatment. All four mutant viruses were much more sensitive than the WT virus to interferon-β inhibition, among which the mutant 10-del exhibited the greatest inhibition (**Fig. 1e**). Collectively, these results suggest that 3′UTR deletions attenuate ZIKV replication through diminished viral RNA synthesis and increased vulnerability to type-1-interferon inhibition.

We tested the stability of mutant viruses by passaging them on Vero cells (an approved cell line for vaccine production[19]). The fifth-passage (P5) viruses developed larger infectious foci (**Supplementary Fig. 3a**) and faster replication kinetics than the corresponding P0 viruses on Vero cells (compare **Supplementary Fig. 3b** with **Fig. 1c**). Complete genome sequencing of P0 and P5 viruses showed that all mutants retained the original deletions, but that the P5 viruses had accumulated additional mutations in the E- and/or NS1-encoding genes (**Supplementary Fig. 3c**), which, we hypothesize, were Vero-cell-adaptive mutation(s) and/or compensatory mutation(s) to 3′UTR deletions. Further passaging of the mutant viruses on Vero cells to P20 did not change the engineered 3′UTR deletions (data not shown), which indicates that the deletions are stable in cell culture.

We evaluated the immunogenicity and efficacy of the 3′UTR-deletion viruses in an A129 mouse model, which is deficient in interferon-α/β receptors[20] (**Fig. 2a**). After subcutaneous (s.c.) inoculation with 1×10^4 IFU of virus, mice infected with the WT virus experienced significantly more weight loss than those infected with a mutated strain, and the four mutant-infected mice showed some, albeit statistically insignificant, weight loss when compared with the mock-infected animals (**Fig. 2b**). About 50% of the mice succumbed to the WT-virus infection, whereas no mortality was observed among mice infected with the mutated strains (**Fig. 2c**). The WT virus produced significantly higher peak viremia than the mutant viruses, among which the 10-del virus had the lowest viremic profile (**Fig. 2d**). The viremia for the 10-del mutant dropped to 700 IFU, 350 IFU, and undetectable levels on days 5, 6, and 7 after infection, respectively (data not shown). Sequencing analysis confirmed that the engineered deletions were retained without other *de novo* mutations in the mutant viruses recovered from the mouse sera (data not shown). On day 28 post-infection, mouse sera were quantified for prechallenge antibody-neutralization titers using an mCherry ZIKV (**Supplementary Fig. 4**). Comparable prechallenge neutralization titers of $(1.8 \pm 1.1) \times 10^3$ to $(8.6 \pm 1.5) \times 10^3$ dilution folds were observed among mice infected with the WT and mutant virus strains (**Fig. 2e**). After challenge with 1×10^5 IFU of WT ZIKV (Cambodian strain FSS13025) on day 28 after immunization, the immunized mice had no detectable peripheral viremia, whereas the mock-immunized group produced a mean viremia of $(8.5 \pm 1.5) \times 10^6$ IFU/ml on day 2 after challenge (**Fig. 2f**). On day 28 after challenge, we measured the neutralization titers of the mouse sera again; notably, the postchallenge neutralization titers were equivalent to the prechallenge neutralization titers (compare **Fig. 2e**,**g**), which suggests that a sterilizing antibody response had been achieved by a single vaccination. All together, the results demonstrate that the mutated viruses are highly attenuated, immunogenic, and protective in A129 mice.

Because the 10-del virus produced the lowest viremia in mice (**Fig. 2d**), yet induced a neutralizing antibody response comparable to those of the WT and other mutants (**Fig. 2e–g**), we prioritized this mutant for further characterization. At a dose of 100 IFU, 10-del-virus-infected mice showed a delayed peak viremia that was about 100-fold lower than that of the WT virus (**Supplementary Fig. 5a**). Equivalent levels of prechallenge neutralizing antibody titers were induced by the WT and 10-del viruses (**Supplementary Fig. 5b**), which led to complete protection from viremia after challenge with 1×10^6 IFU of the Puerto Rican ZIKV strain PRVABC59 (**Supplementary Fig. 5c**). Furthermore, even when immunized at a dose of only

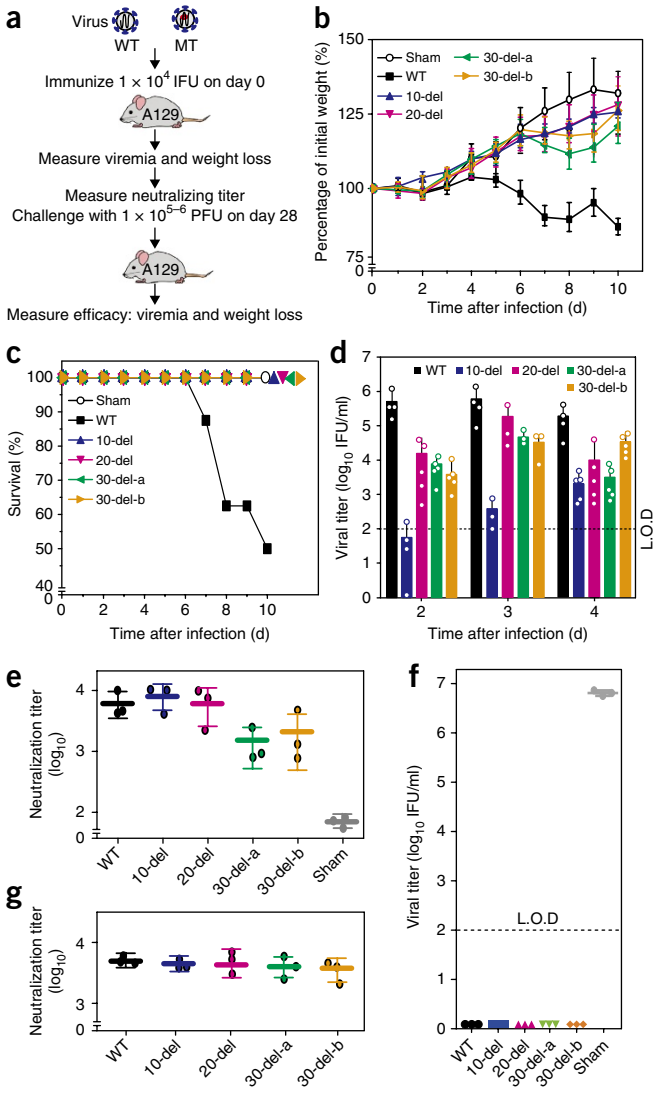

Figure 2 Characterization of 3′UTR mutants in the A129 mouse model. (**a**) Experimental scheme. In two separate experiments, 3-week-old A129 mice ($n = 8$) were immunized through the s.c. route with 1×10^4 IFU WT and mutant viruses. (**b**–**d**) The immunized mice were monitored for weight loss (**b**), survival (**c**), and viremia (**d**). Weight loss is indicated by percentage, using the weight on the day before immunization to define 100%. Viremias were quantified by an immunostaining focus assay from days 2 to 4 post-infection. (**e**) Prechallenge neutralization antibody titers. On day 28 after immunization, mouse sera was measured for neutralizing titers using an mCherry ZIKV infection assay (**Supplementary Fig. 4**). (**f**) Postchallenge viremia. On day 28 after immunization, mice were challenged with 1×10^5 PFU parental virus (ZIKV strain FSS13025) through the i.p. route. Viremia on day 2 after challenge was quantified using the immunostaining focus assay. (**g**) Postchallenge neutralization antibody titer. On day 28 after challenge, mouse sera was quantified for neutralizing titers using the mCherry ZIKV infection assay. L.O.D., limit of detection. Error bars represent s.d.

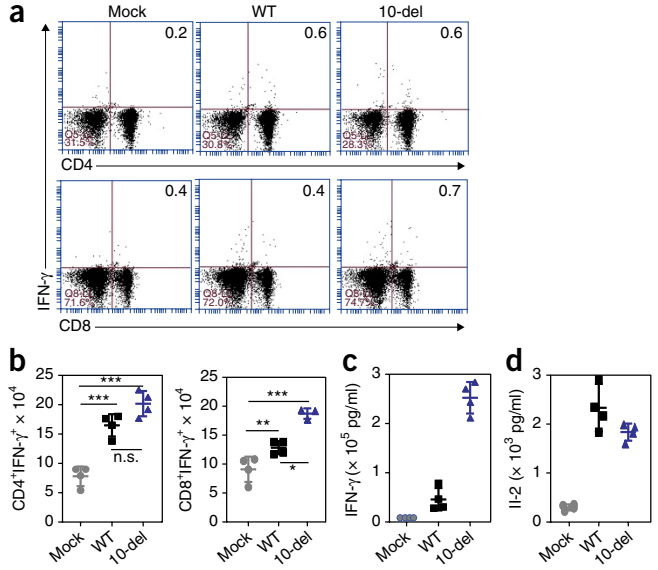

Figure 3 T cell responses after primary infection with WT ZIKV or the 10-del mutant. (**a**) A129 mice were infected with 1×10^4 IFU WT and 10-del viruses. On day 28 after infection, mouse spleens were harvested. Splenocytes were counted, cultured *ex vivo* with WT ZIKV for 24 h, and stained for markers (IFN-γ, CD3, and CD4 or CD8). The T cells were gated, and percentages of $CD4^+IFN\text{-}\gamma^+$ cells and $CD8^+IFN\text{-}\gamma^+$ cells are shown. (**b**) Total number of T cell subsets per spleen. (**c**,**d**) Supernatants from the *ex vivo* culture were harvested on day 2 after WT-ZIKV restimulation and measured for IFN-γ (**c**) and IL-2 (**d**) production. Data are presented as means ± s.e.m., $n = 2$–4 per group. $^*P < 0.05$, $^{**}P < 0.01$, or $^{***}P < 0.001$ difference between the virus- and mock-infected mice.

10 IFU, 10-del-virus-infected mice generated a neutralization titer of $(9.7 \pm 6.8) \times 10^3$ dilution folds and were fully protected from viremia after challenge (**Supplementary Fig. 6**). It is noteworthy that different doses of 10-del mutant (10–10^4 IFU) induced similar neutralization antibody titers and completely prevented viremia upon challenge, demonstrating that the 10-del virus is a potent vaccine candidate.

Given that P5 virus accumulated Vero-cell-adaptive mutations (**Supplementary Fig. 3c**), we compared the virulence and immunogenicity between the P0 and P5 10-del viruses in the A129 mice. After immunization with 100-IFU virus through the s.c. route, the P0 and P5 10-del viruses generated comparable viremia and induced equivalent neutralization titers (**Supplementary Fig. 7a**,**b**). After challenge with 1×10^6 IFU of the Puerto Rican strain PRVABC59 ZIKV through the intraperitoneal (i.p.) route, no viremia was detected in mice vaccinated with the P0 or P5 virus; by contrast, robust viremia was detected in the sham group (**Supplementary Fig. 7c**). These results indicate that the Vero-cell-adaptive mutations recovered from the P5 virus do not substantially affect the virulence and immunogenicity of the 10-del virus in A129 mice.

We analyzed the T cell responses in A129 mice immunized with 1×10^4 IFU of WT and 10-del viruses. On day 28 postimmunization, ZIKV-specific T cells from the spleen were restimulated with live WT virus *in vitro*, and analyzed using an intracellular cytokine staining (ICS) assay and a Bio-Plex immunoassay. The results showed that both WT- and mutant-virus immune $CD4^+$ and $CD8^+$ T cells had higher interferon (IFN)-γ responses than the mock-immunized group (**Fig. 3a**,**b**). Furthermore, total immune T cells induced more IFN-γ (**Fig. 3c**) and interleukin (IL)-2 (**Fig. 3d**) than those in the mock group; notably, T cells immunized with the 10-del mutant produced four-fold higher levels of IFN-γ than cells immunized with the WT virus (**Fig. 3c**). These results indicate that the 10-del vaccine candidate induces a robust T cell response.

Three sets of experiments were performed to analyze the safety of the 10-del vaccine candidate. First, we measured the viral loads in different organs after s.c. inoculation of A129 mice with 1×10^4

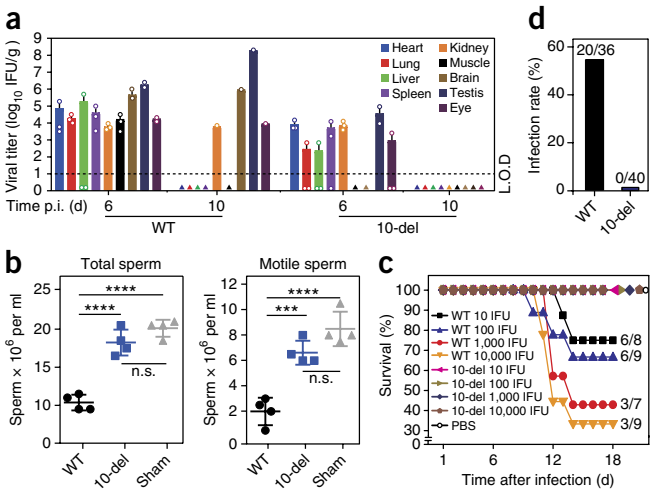

Figure 4 Safety evaluation of 10-del virus. (**a**) Viral loads in organs of infected A129 mice. 3-week-old A129 mice were immunized with 1×10^4 IFU of WT and 10-del viruses. Organs from infected mice were collected and homogenized on days 6 and 10 postinfection (p.i.). The amounts of viruses were quantified on Vero cells using an immunostaining focus assay. The mean ± s.e.m. results from three animals are presented in each group. Triangle symbols denote no detectable virus. (**b**) Sperm-count analysis of A129 mice infected with WT or 10-del mutant virus. Male A129 mice were infected with 1×10^4 IFU of WT and 10-del viruses ($n = 4$ per group). On day 16 p.i., the epididymis was harvested for sperm-count analysis. Total sperm counts and motile-sperm counts are shown. A one-way analysis of variance (ANOVA) test was performed to indicate statistical significance among different infection groups. n.s., not significant, $^{***}P < 0.001$, $^{****}P < 0.0001$. (**c**) Comparison of neurovirulence of WT and 10-del viruses in CD-1 newborn mouse. Groups of 1-d-old CD-1 mice ($n = 7$–10, as indicated) were injected with 10 to 10,000 IFU of WT or 10-del virus through the i.c. route. Survival numbers and total number of infected animals were calculated. Survival percentages of infected mice are presented. (**d**) Mosquito infectivity assay. *Aedes aegypti* were fed with WT or 10-del virus on artificial-blood meals. On day 7 after feeding, individual engorged, incubated mosquitoes were homogenized and infection was assayed by immunostaining of viral-protein expression on inoculated Vero cells. The numbers of infected mosquitoes and total numbers of engorged mosquitoes are indicated.

IFU of WT or 10-del viruses (**Fig. 4a**). On day 6 after infection, WT-infected mice had high viral loads in all organs tested, whereas the 10-del-infected mice had no virus in muscle or brain and lower viral loads in the heart, lung, liver, spleen, kidney, testes, and eye. The results suggest organ-selective attenuation of the 10-del virus. On day 10 after infection, mice infected with the WT virus retained viral loads in kidney, brain, testis, and eye, among which the testes had the highest mean titer; by contrast, no virus ($\leq 10^2$ IFU/ml) could be detected in any organs from the 10-del-infected mice. Because ZIKV infection was reported to damage the testis in mice[21,22], we examined the effect of immunization on the function of the testes in the A129 mice. On day 16 after immunization, similar weight and size of testes were observed in mice infected with the mock, WT, and 10-del mutant viruses (data not shown). However, total sperm counts and motile-sperm counts were reduced in mice infected with the WT virus, whereas mice infected with the 10-del virus did not have significantly compromised sperm counts (**Fig. 4b**). Second, we examined the neurovirulence of the 10-del virus through intracranial (i.c.) injection of 1-d-old CD-1 mice (**Fig. 4c**). The newborn mice succumbed to WT virus infection in a dose-responsive manner; even a dose of 10 IFU resulted in 25% mortality. By contrast, no mice infected with the 10-del virus died, even at a dose of 1×10^4 IFU. Finally, we determined whether the 10-del virus could infect *Aedes aegypti* mosquitoes, the main transmission vector of ZIKV in the Americas[23,24]. After exposure to artificial-blood meals containing 1×10^6 IFU/ml of WT or 10-del virus, and incubation for 7 d, 56% of the engorged mosquitoes were infected by the WT virus, whereas no mosquitoes were infected by the 10-del mutant (**Fig. 4d**). Furthermore, an intrathorax injection of the 10-del virus into mosquitoes did not yield any infectious virus on day 7 after injection (data not shown). Collectively, our results demonstrate that the 10-del virus had substantially reduced or absent viral loads in mouse organs, decreased neurovirulence by >1,000-fold, compared to WT virus and failed to infect the principal urban mosquito, all of which are suggestive of an excellent safety profile.

A successful vaccine requires a fine balance between efficacy and safety. Live-attenuated vaccines generally offer fast and durable immunity, but sometimes, with the trade-off of reduced safety, whereas inactivated and subunit vaccines often provide enhanced safety but may require multiple doses and periodic boosters. Our data indicate that the 3′UTR-10-del ZIKV is a promising live-attenuated vaccine candidate with a good balance between efficacy and safety. A single immunization elicited robust antibody and T cell responses and induced sterilizing immunity in mice against epidemic ZIKV strain. Vaccine-induced sterilizing immunity is thought to be crucial for a ZIKV vaccine to successfully prevent viremia and congenital abnormalities. The safety profile of this vaccine candidate is highlighted by the low viremia, little and transient viral loads in organs, and limited weight loss in the immunodeficient A129 mouse model, as well as the lack of mortality among 1-d-old immunocompetent CD-1 mice after receiving an i.c. injection. In comparison, i.c. inoculation with the YFV 17D and JEV SA14-14-2 vaccines—two licensed, live-attenuated flavivirus vaccines—causes deaths in 1-d-old mice[25,26]. Although potential homologous recombination between WT ZIKV and the 10-del-virus vaccine may pose a safety liability, it should be noted that recombination events are rare and could not be detected in cell cultures for West Nile virus (WNV) and DENV[27–31]. As compared to chimeric vaccines, live-attenuated ZIKV vaccines—for example, YFV 17D expressing ZIKV prM-E, or DENV expressing ZIKV prM-E[32]—our 3′UTR-mutant-virus vaccine has the advantage of retaining all ZIKV structural and nonstructural genes that might contribute to antiviral protection, as indicated by DENV studies[33,34]. Mechanistically, the 3′UTR mutant viruses seemed to be attenuated through decreased viral RNA replication and increased sensitivity to type-1-interferon inhibition. The latter mechanism is in agreement with the observation that genetic diversity at the 3′UTR of DENV contributes to epidemic potential[18]. Future studies are needed to investigate why 20-del and 30-del mutants were less attenuated than the 10-del mutant, and how the attenuation strategy discovered in ZIKV could be applied to the development of other flavivirus vaccines. Taken together, our results indicate that the 3′UTR mutant ZIKV is an attractive vaccine candidate that should be advanced to nonhuman primates for further development.

METHODS

Methods, including statements of data availability and any associated accession codes and references, are available in the online version of the paper.

Note: Any Supplementary Information and Source Data files are available in the online version of the paper.

ACKNOWLEDGMENTS
We thank colleagues at the University of Texas Medical Branch for their helpful discussions during the course of this study. We are grateful to M.A. Garcia-Blanco and S.S. Brarick for providing lab space and equipment during the early stage of this work. P.-Y.S. was supported by a University of Texas Medical Branch (UTMB) start-up award, UTMB Innovation and Commercialization award, University of Texas STARs Award, CDC grant for the Western Gulf Center of Excellence for Vector-Borne Diseases, Pan American Health Organization grant SCON2016-01353, and UTMB CTSA UL1TR-001439. This research was also partially supported by a US National Institutes of Health grant AI120942 to S.C.W.

AUTHOR CONTRIBUTIONS
C.S., A.E.M., B.T.D.N., H.L., X.X., and D.B.A.M. performed experiments and data analysis. M.W., R.B.T., A.D.B., S.C.W., P.F.C.V., T.W., S.L.R., and P.-Y.S. designed the experiments and interpreted the results. C.S., A.E.M., T.W., S.C.W., P.F.C.V., S.L.R., and P.-Y.S. wrote the manuscript.

COMPETING FINANCIAL INTERESTS
The authors declare competing financial interests: details are available in the online version of the paper.

1. Costello, A. *et al.* Defining the syndrome associated with congenital Zika virus infection. *Bull. World Health Organ.* **94**, 406–406A (2016).
2. Weaver, S.C. *et al.* Zika virus: History, emergence, biology, and prospects for control. *Antiviral Res.* **130**, 69–80 (2016).
3. Shan, C. *et al.* Zika virus: diagnosis, therapeutics, and vaccine. *ACS Infect. Dis.* **2**, 170–172 (2016).
4. Dawes, B.E. *et al.* Research and development of Zika virus vaccines. *npj Vaccines* **1**, 16007 (2016).
5. Barrett, A.D.T. Zika vaccine candidates progress through nonclinical development and enter clinical trials. *Npj Vaccines* **1**, 16023 (2016).
6. Larocca, R.A. *et al.* Vaccine protection against Zika virus from Brazil. *Nature* **536**, 474–478 (2016).
7. Dowd, K.A. *et al.* Rapid development of a DNA vaccine for Zika virus. *Science* **354**, 237–240 (2016).
8. Abbink, P. *et al.* Protective efficacy of multiple vaccine platforms against Zika virus challenge in rhesus monkeys. *Science* **353**, 1129–1132 (2016).
9. Richner, J.M. *et al.* Modified mRNA vaccines protect against Zika virus infection. *Cell* **168**, 1114–1125.e10 (2017).
10. Pardi, N. *et al.* Zika virus protection by a single low-dose nucleoside-modified mRNA vaccination. *Nature* **543**, 248–251 (2017).
11. Whitehead, S.S. Development of TV003/TV005, a single dose, highly immunogenic live attenuated dengue vaccine; what makes this vaccine different from the Sanofi-Pasteur CYD™ vaccine? *Expert Rev. Vaccines* **15**, 509–517 (2016).
12. Shan, C. *et al.* An infectious cDNA clone of Zika virus to study viral virulence, mosquito transmission, and antiviral inhibitors. *Cell Host Microbe* **19**, 891–900 (2016).
13. Akiyama, B.M. *et al.* Zika virus produces noncoding RNAs using a multi-pseudoknot structure that confounds a cellular exonuclease. *Science* **354**, 1148–1152 (2016).
14. Ye, Q. *et al.* Genomic characterization and phylogenetic analysis of Zika virus circulating in the Americas. *Infect. Genet. Evol.* **43**, 43–49 (2016).
15. Lo, M.K., Tilgner, M., Bernard, K.A. & Shi, P.-Y. Functional analysis of mosquito-borne flavivirus conserved sequence elements within 3′ untranslated region of West Nile virus by use of a reporting replicon that differentiates between viral translation and RNA replication. *J. Virol.* **77**, 10004–10014 (2003).
16. Xie, X. *et al.* Zika virus replicons for drug discovery. *EBioMedicine* **12**, 156–160 (2016).
17. Pijlman, G.P. *et al.* A highly structured, nuclease-resistant, noncoding RNA produced by flaviviruses is required for pathogenicity. *Cell Host Microbe* **4**, 579–591 (2008).
18. Manokaran, G. *et al.* Dengue subgenomic RNA binds TRIM25 to inhibit interferon expression for epidemiological fitness. *Science* **350**, 217–221 (2015).
19. World Health Organization. Acceptability of cell substrates for production of biologicals. Report of a WHO Study Group on Biologicals. *World Health Organ. Tech. Rep. Ser.* **747**, 1–29 (1987).
20. Rossi, S.L. *et al.* Characterization of a novel murine model to study Zika virus. *Am. J. Trop. Med. Hyg.* **94**, 1362–1369 (2016).
21. Govero, J. *et al.* Zika virus infection damages the testes in mice. *Nature* **540**, 438–442 (2016).
22. Ma, W. *et al.* Zika virus causes testis damage and leads to male infertility in mice. *Cell* **167**, 1511–1524.e10 (2016).
23. Guerbois, M. *et al.* Outbreak of Zika virus infection, Chiapas State, Mexico, 2015, and first confirmed transmission by *Aedes aegypti* mosquitoes in the Americas. *J. Infect. Dis.* **214**, 1349–1356 (2016).
24. Ferreira-de-Brito, A. *et al.* First detection of natural infection of Aedes aegypti with Zika virus in Brazil and throughout South America. *Mem. Inst. Oswaldo Cruz* **111**, 655–658 (2016).
25. Yun, S.I. *et al.* Comparison of the live-attenuated Japanese encephalitis vaccine SA14-14-2 strain with its pre-attenuated virulent parent SA14 strain: similarities and differences in vitro and in vivo. *J. Gen. Virol.* **97**, 2575–2591 (2016).
26. Barrett, A.D. & Gould, E.A. Comparison of neurovirulence of different strains of yellow fever virus in mice. *J. Gen. Virol.* **67**, 631–637 (1986).
27. Khromykh, A.A., Sedlak, P.L. & Westaway, E.G. trans-Complementation analysis of the flavivirus Kunjin ns5 gene reveals an essential role for translation of its N-terminal half in RNA replication. *J. Virol.* **73**, 9247–9255 (1999).
28. Khromykh, A.A., Kenney, M.T. & Westaway, E.G. trans-Complementation of flavivirus RNA polymerase gene NS5 by using Kunjin virus replicon-expressing BHK cells. *J. Virol.* **72**, 7270–7279 (1998).
29. Qing, M., Liu, W., Yuan, Z., Gu, F. & Shi, P.Y. A high-throughput assay using dengue-1 virus-like particles for drug discovery. *Antiviral Res.* **86**, 163–171 (2010).
30. Xie, X., Zou, J., Puttikhunt, C., Yuan, Z. & Shi, P.Y. Two distinct sets of NS2A molecules are responsible for dengue virus RNA synthesis and virion assembly. *J. Virol.* **89**, 1298–1313 (2015).
31. Pugachev, K.V. *et al.* High fidelity of yellow fever virus RNA polymerase. *J. Virol.* **78**, 1032–1038 (2004).
32. Xie, X. *et al.* Understanding Zika virus stability and developing a chimeric vaccine through functional analysis. *MBio* **8**, e02134–16 (2017).
33. Yauch, L.E. *et al.* A protective role for dengue virus-specific CD8+ T cells. *J. Immunol.* **182**, 4865–4873 (2009).
34. Weiskopf, D. *et al.* Comprehensive analysis of dengue virus-specific responses supports an HLA-linked protective role for CD8+ T cells. *Proc. Natl. Acad. Sci. USA* **110**, E2046–E2053 (2013).

ONLINE METHODS

Cells, viruses, and antibodies. Vero cells were purchased from the American Type Culture Collection (ATCC; Bethesda, MD) and cultured at 37 °C with 5% CO_2 in a high-glucose Dulbecco modified Eagle's medium (DMEM; Invitrogen, Carlsbad, CA) with 10% FBS (FBS; HyClone Laboratories, Logan, UT) and 1% penicillin/streptomycin (Invitrogen, Carlsbad, CA). The following antibodies were used: a mouse monoclonal antibody (mAb) 4G2 that is cross-reactive with flavivirus E protein (ATCC), ZIKV-specific HMAF (hyperimmune ascitic fluid; obtained from the World Reference Center of Emerging Viruses and Arboviruses (WRCEVA) at the University of Texas Medical Branch), anti-mouse IgG antibody labeled with horseradish peroxidase (KPL, Gaithersburg, MD), and goat anti-mouse IgG conjugated with AlexaFluor 488 (Thermo Fisher Scientific). The ZIKV Cambodian strain FSS13025 (GenBank number KU955593.1) was produced from an infectious cDNA clone pFLZIKV[12]. The Puerto Rican strain PRVABC59 (GenBank number KU501215) was obtained from WRCEVA. All cell lines tested negative for mycoplasma. Antibody 4G2, ZIKV-specific HMAF, anti-mouse IgG, and goat anti-mouse IgG conjugated with AlexaFluor 488 were diluted 1:40, 1:2,000, 1:2,000 and 1:1,000 folds, respectively, in the indicated assays.

Plasmid construction. To engineer 3′UTR deletions, overlap PCR containing the deletions was performed to amplify the DNA fragment between unique restriction-enzyme sites EcoRI and ClaI. The DNA fragments containing the 3′UTR deletions were individually introduced into the pFLZIKV and pZIKV Rep (replicon cDNA plasmid[16]) through the EcoRI and ClaI sites. The construction of the cDNA clone for mCherry ZIKV will be reported elsewhere. DNA sequencing was performed to verify all the constructs. All restriction enzymes were purchased from New England BioLabs (Ipswitch, MA). Primer sequences are available upon request.

RNA transcription and transfection. Genomic ZIKV, mCherry ZIKV, and replicon RNAs were transcribed *in vitro* using a T7 mMessage mMachine kit (Ambion, Austin, TX) from corresponding cDNA plasmids prelinearized by restriction enzyme ClaI. The RNA was precipitated with lithium chloride, washed with 70% ethanol, resuspended in RNase-free water, quantitated by spectrophotometry, and stored at −80 °C in aliquots. The RNA transcripts (10 μg) were electroporated into Vero cells following a protocol described previously[35].

Indirect immunofluorescence assays (IFA). After transfection with genomic RNA, Vero cells were grown in an eight-well Lab-Tek chamber slide (Thermo Fisher Scientific, Waltham, MA). At the indicated time points, the transfected cells were fixed in 100% methanol at −20 °C for 15 min. After 1 h of incubation in a blocking buffer (containing 1% FBS and 0.05% Tween-20 in PBS), the cells were treated with a mouse monoclonal antibody 4G2 for 1 h and washed three times with PBS (5 min for each wash). The cells were further incubated with a goat anti-mouse IgG conjugated with AlexaFluor 488 for 1 h in blocking buffer, after which the cells were washed three times with PBS. The slides were mounted in a mounting medium with DAPI (4′, 6-diamidino-2-phenylindole; Vector Laboratories) and analyzed under a fluorescence microscope equipped with a video-documentation system (Olympus).

Luciferase assay. The luciferase assay was performed as previously reported[16]. Briefly, Vero cells were transfected with 10 μg of WT or mutant ZIKV replicon RNAs and seeded in a 12-well plate. At the indicated time points, the cells were washed once with PBS and lysed using cell-lysis buffer (Promega, Madison, WI). The lysed cells were scraped from plates and stored at −80 °C. The luciferase signals were quantified by Cytation 5 (Biotek) following the manufacturer's instructions.

Stability of 3′UTR mutants, RNA extraction, and RT–PCR. To examine the stability of 3′UTR mutants, we passaged the viruses on Vero cells for twenty rounds. T-25 flasks were seeded with 1.5×10^6 Vero cells per flask. The viruses derived from RNA transfection, defined as P0, were used to infect the Vero cells. At 5 d p.i., 100 μl of culture fluid was transferred to a new T-25 flask containing naive Vero cells in 5 ml of culture medium. After five rounds or twenty rounds of such passaging (P5 and P20), QIAamp Viral RNA Kit (Qiagen) was used to extract viral RNAs from the culture fluids. SuperScript III one-step RT–PCR kits (Invitrogen) was used to amplify viral RNAs. The RT–PCR products were subjected to DNA sequencing. Three independent passages were performed for each mutant virus.

Immunostaining focus assay and immunostaining. An immunostaining focus assay was performed by serial tenfold dilutions (10^1–10^6) of viral samples in DMEM. For each dilution, 100 μl of sample was added to a 24-well plate containing 90% confluent Vero cells. The infected cells were swirled every 15 min to ensure complete coverage of the cell monolayer for even infection. After 1 h incubation, we added into each well 0.5 ml of methyl cellulose overlay containing 2% FBS 1% penicillin/streptomycin. The plate was incubated at 37 °C for 4 d, after which the methyl cellulose overlay was removed, 0.5 ml methanol–acetone (1:1) fixation solution was added per well, and the plate was incubated for 15 min at room temperature. After removing the fixation solution, the plates were air dried, washed three times with PBS, incubated in buffer (PBS with 3% FBS) for 1 h, and reacted with ZIKV-specific HMAF for 1 h. The plates were washed three times with PBS, incubated for 1 h with the horseradish peroxidase-conjugated secondary antibody (KPL, Gaithersburg, MD), and detected for immunofocusing through the addition of aminoethylcarbazole substrate, following the manufacturer's instructions (ENZO Life sciences, Farmingdale, MA).

Viral-replication analysis. Vero cells in 12-well plates (80% confluent) were infected with either P0 or P5 ZIKV at an MOI of 0.01 in duplicate wells. Viral stocks were diluted to appropriate concentrations in DMEM containing 2% FBS and 1% penicillin/streptomycin and added to infect cells (100 μl of virus per well). The inoculants were removed after 1 h infection at 37 °C. The cell monolayers were washed three times with PBS, and 1 ml DMEM medium containing 2% FBS and 1% penicillin/streptomycin was added to each well. The medium was collected daily for immunostaining focus assay as described above.

Vaccination and challenge of mice. All animal experiments were approved by the University of Texas Medical Branch IACUC. A129 mice were obtained from colonies maintained under specific pathogen-free conditions at University of Texas Medical Branch. 3-week-old A129 mice were infected with 1×10^4 IFU, 1×10^2 IFU, or 10 IFU WT or mutant viruses through the s.c. route. PBS was given to the mock-infected mice through the same route. Disease progression of mice was monitored by weight loss and deaths. To measure viremia, mice were anesthetized and bled through the retro-orbital sinus (r.o.) every other day. On day 28 p.i., mice were measured for neutralizing antibody titers using an mCherry ZIKV infection assay. The immunized mice were then challenged through the i.p. route with either 1×10^5 IFU of FSS13025 or 1×10^6 IFU of PRVABC59 ZIKV, and measured for viremia on day 2 after challenge. Serum was collected by centrifuging the blood at 3,380*g* for 5 min and stored it at −80 °C. Viral titers were determined by an immunostaining focus assay on Vero cells, as described above.

Neurovirulence on newborn CD-1 mice. Groups of 1-d-old outbred CD-1 mice (n = 7–10; Charles River Laboratories) were injected i.c. with WT or 10-del with serial tenfold dilutions from 10,000 IFU to 10 IFU. Mice were monitored daily for morbidity and mortality.

Organ virus titers. A129 mouse organs were removed and measured for viral loads on days 6 and 10 p.i. after vaccination with 1×10^4 IFU of WT and del-10 virus through the s.c. route, as previously described[20].

Testis and sperm-count analyses. A129 mice were infected with 1×10^4 IFU of WT or 10-del mutant virus. A mock-infected group with PBS was included as a negative control. On day 16 p.i., the mice were euthanized and necropsied. Epididymis and testes were removed immediately, as previously described[36]. Briefly, the epididymis was placed into 1 ml of prewarmed M2 media at 37 °C. To release the sperm, we cut the epididymis lengthwise six times and incubated the mixture at 37 °C for 10 min with agitation every 2 min. After the incubation,

doi:10.1038/nm.4322

the media was diluted 1:50 into prewarmed M2 media and counted for motile and nonmotile sperm on a hemocytometer.

Antibody-neutralization assay. Neutralizing activity of mouse sera was assessed using an mCherry ZIKV. The sera were two-fold serially diluted starting at 1:100 in DMEM with 2% FBS and 1% penicillin/streptomycin. The diluted sera were incubated with mCherry ZIKV at 37 °C for 2 h. The antibody–virus complexes were added to infect Vero cells in 96-well plates. After 48 h p.i., the infected cells with mCherry fluorescence were quantified by a Cytation 5 Cell Imaging Multi-Mode Reader (Biotek). The percentage of fluorescence-positive cells in the mock-treatment controls was set at 100%. The fluorescence-positive cells from serum-treated wells were normalized to those of mock-treatment controls. A four-parameter sigmoidal (logistic) model in the software GraphPad Prism 7 was used to calculate the neutralization titers (NT_{50}).

Experimental infection of mosquitoes with ZIKV. *Aedes aegypti* mosquitoes (derived from a Galveston, Texas, colony) were used for blood-meal feeding experiments, as reported previously[12]. The infection rate was defined as the percentage of virus-positive mosquitoes from the total number of engorged mosquitoes[12].

Bio-Plex immunoassay. Approximately 3×10^5 splenocytes were plated in 96-well plates and stimulated with 1.25×10^4 IFU ZIKV strain FSS13025 for 48 h. Culture supernatants were harvested, and cytokine production were measured using a Bio-Plex Pro Mouse Cytokine Assay (Bio-Rad, Hercules, CA).

Intracellular cytokine staining (ICS). Approximately 2.5×10^6 splenocytes were stimulated with 1×10^5 IFU live ZIKV (strain FSS13025) for 24 h. During the final 5 h of stimulation, BD GolgiPlug (BD Bioscience) was added to block protein transport. Cells were stained with antibodies for CD3, CD4, or CD8; fixed in 2% paraformaldehyde; and permeabilized with 0.5% saponin before the addition of anti-IFN-γ, or control rat IgG1 (e-Biosciences). Samples were processed with a C6 Flow Cytometer instrument. Dead cells were excluded on the basis of forward and side light scatter. Data were analyzed with a CFlow Plus Flow Cytometer (BD Biosciences).

Data analysis. All data were analyzed using GraphPad Prism v7.02 software. Data are expressed as means ± s.e.m. Comparisons of groups were performed using one-way ANOVA. A P value of <0.05 indicates statistical significance.

Data availability. Supplementary information and source data used to generate **Figures 1–4** are available in the online version of the paper. Any other information is available upon request.

35. Shi, P.Y., Tilgner, M., Lo, M.K., Kent, K.A. & Bernard, K.A. Infectious cDNA clone of the epidemic west nile virus from New York City. *J. Virol.* **76**, 5847–5856 (2002).
36. Hansen, D.A., Esakky, P., Drury, A., Lamb, L. & Moley, K.H. The aryl hydrocarbon receptor is important for proper seminiferous tubule architecture and sperm development in mice. *Biol. Reprod.* **90**, 8 (2014).